J. Water Environ. Nanotechnol., 6(1): 11-21 Winter 2021

ORIGINAL RESEARCH PAPER

New metal organic framework (MOF) nanoparticle for gas separation by matrix membranes

Seyed Hamed Mousavi[2],Fatemeh Ajoudani[2],Taher Yousefi[1,*], Amir Charkhi[1], Nima Rezaee Mojdehi[2], Ramin Yavari[1]

[1] Nuclear Science and Technology Research Institute (NSTRI), P.O. Box. 11365-8486, Tehran, Iran
[2] Separation Process and Nanotechnology Lab, Faculty of Caspian, College of Engineering , University of Tehran, Tehran, Iran

Received: 2020-09-04 Accepted: 2020-10-14 Published: 2021-02-01

ABSTRACT

{[Dy(BTC)(H_2O)]·DMF}n metal-organic framework nanoparticles were synthesized through the solvothermal method. The product was characterized by XRD, TG, BET, and SEM techniques. SEM images showed that the synthesized sample has semi-cubic particles with an average size of 70 nm in length. To improve the gas separation performance; the MOF nanoparticles were dispersed in polydimethylsiloxane (PDMS) for the preparation of a mixed matrix membrane (MMM) on the support of polyethersulphone (PES). The obtained MMM performance in the separation of NO, N_2, and O_2 gas was investigated and the effect of MOF nanoparticles (5, 10, and 15% wt) and feed pressure (100-250 kPa) on permeability and selectivity were studied. It was found that the membrane performance was evaluated by the addition of MOF nanoparticles in the membrane (polymeric matrix), and the feed pressure has no important effect on the separation. The performance (NO/N_2 and NO/O_2 selectivity) increased as the loading of MOF particles (up to 15% wt) dispersed within the polymer matrices.

Keywords: *Metal-Organic Framework (MOF); Mixed Matrix Membrane (MMM); Separation; Nanoparticles; Permeability; Selectivity*

How to cite this article
Mousavi S.M.,Ajoudani F., Yousefi T., Charkhi A., Rezaee Mojdehi N., Yavari R. New metal organic framework (MOF) nanoparticle for gas separation by matrix membranes . J. Water Environ. Nanotechnol., 2021; 6(1): 11-21.
DOI: 10.22090/jwent.2021.01.002

INTRODUCTION

Compounds such as NO_x, SO_x, CO, H_2S, NH_3, HCN or organothiols, hydrocarbons, volatile organic compounds (benzene, toluene, methanol, etc.) are concerned as important air pollutants. Human activities are the main sources of these gases [1]. The SO_2, NO_2, and CO emissions during the burning of fossil fuels in the energy consumption process, and the release of toxic pollutant gas during chemical reaction and leak of gas are examples of anthropogenic activities [1]. The photochemical smog and acid rain are the major NO_x threats to health and the environment [1]. Oxidation of atmospheric molecules such as nitrogen and oxidation of nitrogen-containing compounds in the fuel are sources of NO in the combustion process [2].

Studies indicated that nitric oxide, NO, is the major nitrogen oxide emitted in the coal-fired process. Irritation of the eyes and throat, tightness of the chest, nausea, headache, and the gradual loss of strength are the toxic effects of NO on humans. Prolonged exposure to NO could be fatal and could cause violent coughing, difficulty in breathing, and cyanosis [3]. The membrane is cost-saving (investment and operating) and a safe method for the removal and separation of NO. The separation of gases by membranes is a continuous and effective technique [4, 5]. Differential permeation through membranes is the base of membrane gas components separation from their mixtures. The differ-

* Corresponding Author Email: *taher_yosefy@yahoo.com*

ence in physical and chemical properties between the membrane and the permeating species has given enough ability to the membrane to transport one component more readily than the other [5]. The selectivity and permeability are criteria for selecting membrane material [6]. Low selectivity led to multi-step separation processes and increasing the complexity and costs of the membrane process. The permeability determines the membrane area or the number of membrane modules needed for the separation process [6]. Polymer membranes have comparatively lower permeability and selectivity than other membranes for gas separations [7]; hence, the worldwide investigation in finding new membrane materials to improve membrane performance is ongoing. The plasticization effects are the main drawbacks of pure polymeric membranes [8]. This effect could be suppressed with crosslinking, through appropriate functional groups or post-treatment of the membrane. Low permeability and selectivity limit the polymeric membranes application and high cost, difficulty in synthesis, and prone to breakage limit the inorganic membranes (with improved selectivity and permeability) usage in gas separation. Mimed matrix membranes (MMMs)] were introduced to overcome the disadvantages of pure polymeric and inorganic membranes [9].

When in the polymeric phase inorganic or inorganic-organic hybrid material (usually nanosize) are impregnated, the Mixed-matrix membranes (MMMs) would be achieved. Mixed-matrix membranes (MMMs) are inorganic or inorganic-organic hybrid material as discrete phases incorporated into a polymeric matrix [10]. Inorganic materials such as zeolitic or metal-organic framework (MOFs) [10] additives do not show any plasticization behavior; due to their interaction with the functional groups of a polymer matrix, MMMs are not only attractive concerning selectivity and permeability but also concerning plasticization resistance. MOFs are a class of inorganic materials with unique properties such as high porosity, large inner surface area, tunable pore sizes, and topologies [11]. MOFs have several advantages over zeolites and porous inorganic materials. An inherent part of MOFs are organic ligands and therefore it causes better interaction of MOF particles with a polymer material and its functionalities (for MMMs, a strong interaction between the two components is very important). Therefore, the gaps between the "inorganic" filler and the organic polymer phase, which leads to a loss in selectivity, could be eliminated. Also, the MOF surface properties could be easily modified (post-treatment) if requested. The higher pore volumes and lower density of MOFs compared with zeolites, and consequently, their effect on the membrane behaviors could be more pronounced for a given mass loading [12].

They could be prepared through a reaction between metal ions and organic ligands [13]. An important advantage of MOFs over porous and other materials is their narrow pore size distribution or identical pore size throughout the whole framework structure. To the best of our knowledge, the synthesis of Dy-BTC MOF and its application for the separation of N_2, O_2, and NO gas has not been reported yet. For research, the Dy-BTC MOF is synthesized by a simple chemical method and incorporated in the polymer matrix to prepare a mixed-matrix membrane for gas separation.

EXPERIMENTAL

Experimental methods comprise different stages such as synthesis of MOF, preparation of pure polymeric and MMMs, characterization of MOF and MMMs, and gas separation.

Materials

$Dy(NO_3)_3.6H_2O$), DMF (C_3H_7NO), 1,3,5-benzenetricarboxylic acid (BTC), tetramethyl ammonium hydroxide, C_2H_5OH, normal hexan, PDMS, Sylgard 184, Crosslinking: (SYLGARD® 184, produced by Dow Corning), PES, and N_2, O_2, and NO gas were of analytical grade and used without further purification.

Synthesis of MOF

MOFs were synthesized by the solvothermal method. Typically, 0.25 mmol of $Dy(NO_3)_3.6H_2O$ and 2 mL DMF were mixed to form solution A. Later on, 0.5 mmol BTC (1,3,5-benzene tricarboxylic acid) and 4 mL DMF were mixed to form solution B. Solutions A and B were mixed and 1 mL water was added. The solution pH was 3.2. About 0.3 mL of tetramethylammonium hydroxide (10%) was added to adjust the pH around 5.46. Afterward, the solution was transferred to a 125 mL Teflon vessel and kept at 100 °C for 17 hours in an air oven and subsequently, it was cooled to room temperature in 6 hours. The prepared sample was rinsed with DMF and ethanol to remove impurities. The solid sample was dried at 160 °C for 30 min. For BET analysis the sample was heated at 300°C for 3 hours.

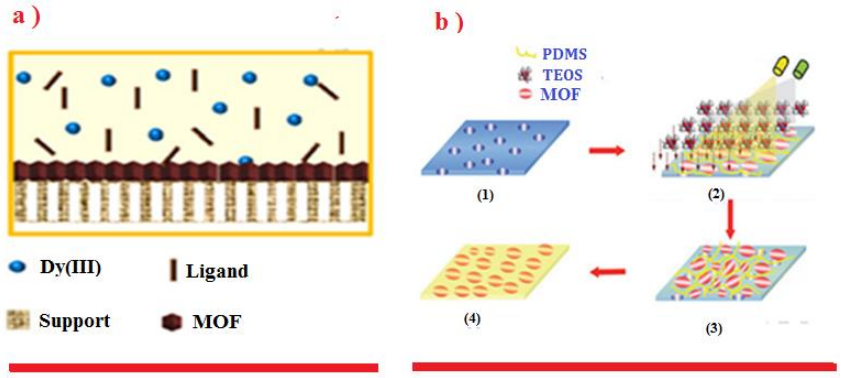

Fig. 1. a) Mechanism of MOF formation on Teflon surface, b) scheme of PES/PDMS-MOF MMM formation.

Characterization

The synthesized sample was analyzed by various methods including SEM, XRD, FTIR and

BET methods. The powder X-ray diffraction pattern was obtained by an STOE STADI MP

diffractometer equipped with monochromatized Cu-Ka radiation (λ = 0.154 nm, 40 kV and

30 mA). Fourier transforms infrared (FT IR) spectrophotometer (Bruker, Vector 22) was used (KBr disks at room temperature) to characterize the synthesized MOF. The Scanning Electron Microscope (SEM) model EM-3200 made by KYKY of China was used to analyze the size distribution and morphology of the nanoparticles. The surface area of the samples was also determined by the BET method on a Quanta chrome Nova2200 nitrogen adsorption apparatus. The samples were degassed in a vacuum chamber for 3 hours at 300 ˚C before BET analysis.

Synthesis of PDMS and PDMS/MOF membrane on the porous PES membrane

The PDMS membrane (30% polymer) was synthesized through the dry phase inversion technique. The Sylgard 184 Silicone Elastomer (Part A) was dissolved inappropriate amounts of n-hexane; later on, the curing agent (Part B) was added to the solution in the 1:10 (part B/part A) ratio. The mixture was stirred for about 30 min and the trapped bubbles in the polymeric solution were consequently removed by sonication of the solution for 15 min. To improve the mechanical strength of PDMS membranes, the PES membrane was used as porous support and the membranes were prepared on it. The pores of PES were filled by soaking in distilled water for about 24 h. Then, the pretreated PES membrane was coated by the PDMS polymeric solution and consequently aired at the ambient temperature for 24 h to evaporate the solvent. Finally, to complete the evaporation and curing process, the heat treatment at 100 ˚C for 2h was performed. To determine the effects of MOF nanoparticles on the gas separation performance of MMM, the various membrane containing the 2.5,5, 10, 15, and 20 wt% of MOF nanoparticles were prepared. The optimum value of polymer to solvent weight was determined based on the obtained value in the PDMS fabrication procedure. Initially, the MOF nanoparticles were dispersed in the n-hexane and ultrasonicated (power 250 w) for about 30 min. Afterward, the curing agent (part B) with the weight ratio of 1:10 (part B/A) was added to the MOF nanoparticles suspension and stirred rigorously for 30 min. Finally, the Sylgard 184 Silicone Elastomer was added to obtain a hemogenic solution. The casting and curing process was performed according to the PDMS fabrication procedure (Fig. 1).

Single gas permeation tests

The gas permeation experiments of pure membrane and MMMs were carried out in batch constant volume module using a variable pressure/ constant volume method. The experimental set up presented in Fig. 2. The effective area of the membrane was 3.44 cm^2. A rotary vane vacuum pump (AdixonTM (AlcatelR) model:1015) was used to evacuate up (to $5*10^{-3}$ mbar) the downstream side of the membrane module. The gaseous feed pressure on the membrane (i.e. feed side) is maintained at a constant level in the range of100–250 kPa. A pressure transmitter (Sensys, model: PTCHC-003BCIA, Accuracy of 0.5% FS) was used for the determination of the permeate gas pressure at various interval times (Fig.2). To ensure the absence of impurity in the module chambers, all the connected paths of the module were evacuated before

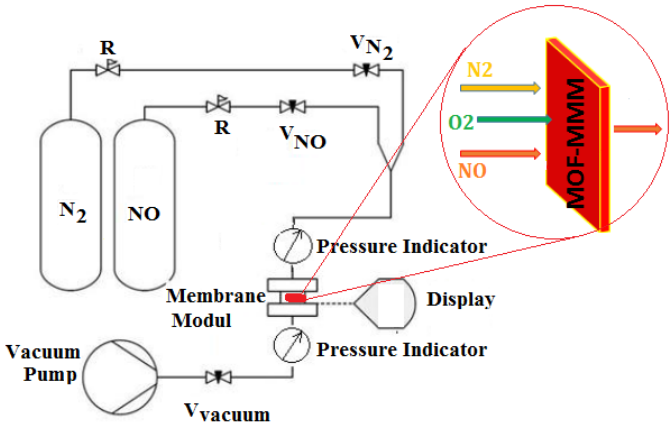

Fig.2. Experimental setup for gas permeation measurements

each experiment. Later on, NO, O_2 or N_2 gas were separately injected into the feed side of the membrane. The mass balance around a control volume covering the permeate side of the module was considered for calculating the permeability (following equation) [14]:

$$\frac{dn}{dt} = J.A = \frac{K.A}{l}\Delta p \quad (1)$$

P: permeability (cm mol/(cm^2 s kPa)), q: permeation flux [mol/(cm^2 s)], A: membrane surface area (cm^2),l: membrane's thickness(cm) Δp: pressure differences of the feed and permeate side (kPa). Assuming the studies gases have ideal gas behavior at the given pressure, Integrating Eq. (1) yields[14]:

$$K = \frac{-l.V}{A.T.R.t}\ln\left(1-\frac{p}{p_0}\right) \quad (2)$$

K; permeability, P: Permeated gas pressure, p_o: Constant feed pressure (kPa), V: volume of permeate side chamber (cm^3). After determining of gases permeability, the ideal selectivity was calculated as follows:

$$S_{i,j} = \frac{K_i}{K_j} \quad (3)$$

RESULTS AND DISCUSSION

TGA, DSC, and BET

The thermogravimetric analysis (TGA) and the differential scanning calorimetry (DSC) of synthesized MOF were obtained at a scan rate of 5˚C/min in air flux (Fig.3 a). The slight weight loss from room temperature to 200˚C (concurrent with a small endotherm peak in the DSC curve) could be assigned to the elimination of the non-coordinative and coordinative water molecules to Dy atoms as well as the evaporation of solvent species [15]. The major weight loss (about 55%) of the sample was observed from 500 to 600 ˚C considering the degradation and burning of the organic moiety of metal-organic framework (BTC) which is concurrent with an intense exothermic peak in the DSC curve. In another word, at above 600 ˚C Dy-BTC convert to Dy_2O_3 by thermal decomposition [15-18].

Surface area and pore volume of the preheated sample at 300°Cat vacuum measured by N_2 adsorption at 77 K (Fig.3b). The heat treatment leads to the evaporation of the solvent and other non-reacted species from the structure of MOF and evacuation of the pores. Also, heat treatment leads to the complete crystallization of MOF.Fig.3b shows the N_2adsorption/desorption isotherms of the synthesized MOF. The sample exhibited type IV isotherms with an H_3 hysteresis loop, which indicates mesoporous structure, the BJH method desorption pore diameter was 2.43 nm (Fig.3, inset) which is in the mesoscale range [19]. The Brunauer-Emmett-Teller (BET) formula was used for the determination of surface area. The surface area was 801.033 m^2/g with a total pore volume of 1300 cc g^{-1} (p/p˚= 0.98). These results are consistent with our prior research[11].

FTIR and XRD

The FTIR spectra of synthesized MOFis shown in Fig.5. The broadband observed above 3300cm^{-1} clears the presence of water molecules in the porous framework. The observed absorption bands below 2000cm $^{-1}$ are belonging to the carboxylate group and the benzene ring which is in line with

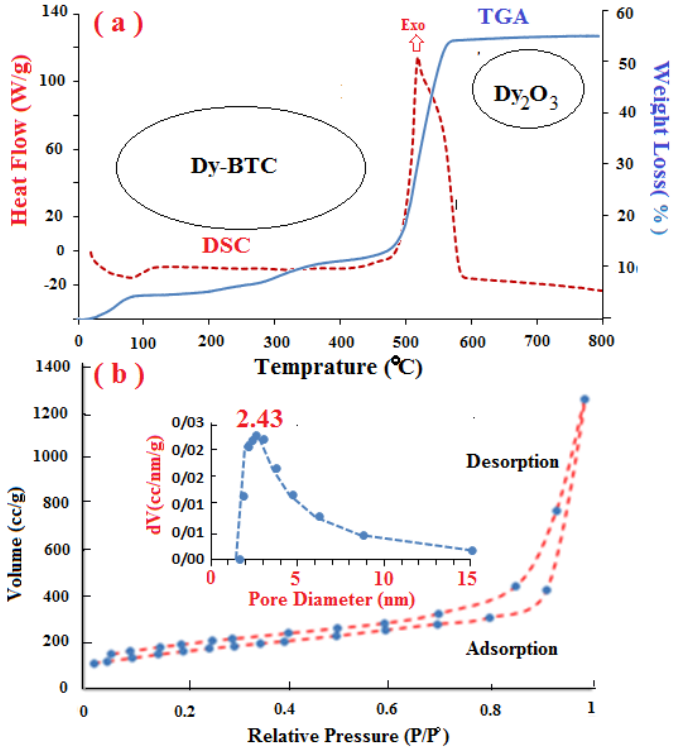

Fig.3. a) TGA and DSC curves, b) N_2 adsorption-desorption isotherm of Dy-BTC MOF (inset: Barrett–Joyner–Halenda (BJH) pore size distribution).

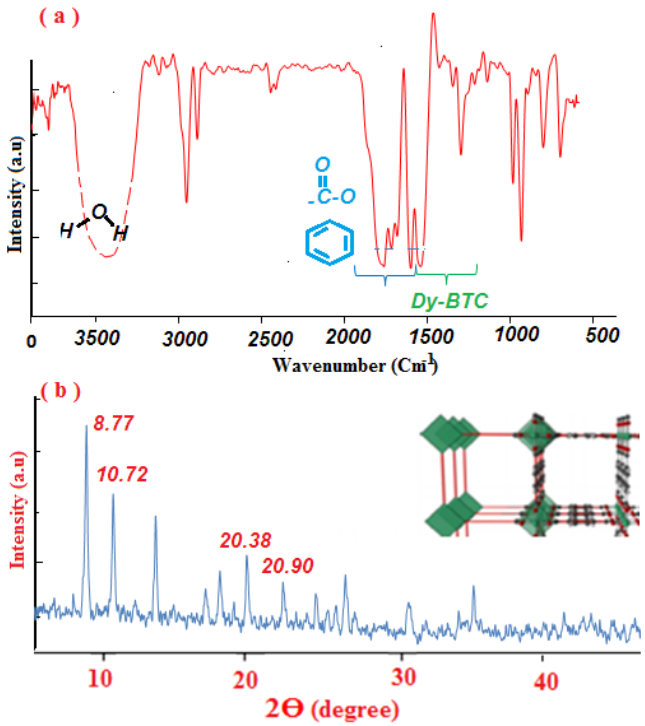

Fig.4. a) FTIR spectra, b) XRD pattern of synthesized MOF sample

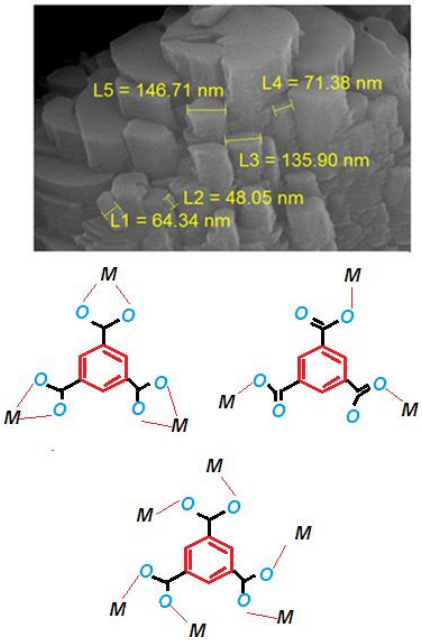

Fig.5 SEM image and X-ray pattern of synthesized MOF sample (inset) The possible configurations of 1,3,5-benzenetricarboxylic acid with metal atoms

the presence of organic ligand in MOF structure. The absorption bands at 1350, 1440, and1620 cm^{-1} can be attributed to Dy-BTCs bonds(metal ion coordinated COO moiety). The observed at bands at1000 and900 cm^{-1}indicating the presence of Dy coordinating to DMF molecules [19].

The XRD pattern of the prepared Dy-BTC-MOF is shown in Fig. 4b and compared with the pattern given in reference [11,20]. The characteristic peaks at Bragg angle of 2Θ =8.77, 10.72, 20.38, and 22.99 are in line with the reference pattern and confirm MOF formation [11, 20].

SEM

The SEM image of the synthesized MOF is shown in Fig.5. Two concomitantly thermodynamic and kinetic factors control and influence the particle morphology. The equilibrium morphology of the final particle is indicated by thermodynamic factors, while the ease with which the thermodynamically favored morphology can be achieved is indicated by the kinetic factors. As can be seen different semi-cubic particles with an average length size of 70 nm are interlocked to form larger particles. The interlocking of cubic and sphere shape particles gives a rock-like or mountain-like appearance to MOF morphology. The possible bond formation between the 1,3,5-benzene tricarboxylic acid and dysprosium metal ions is shown in Fig.5(inset).

Membrane characterization

The surface and cross-section SEM images of the PDMS/PES membranes are shown in Fig. 6(a and b). This image indicates that the prepared PDMS on the PES porous support has a smooth and uniform surface. The SEM images of the MMM with 20wt% loading Dy-BTC are shown in Fig. 6(c,d). As can be seen, the presence of MOF particles in the PDMS matrix changed the surface and cross-section appearance of the membrane. Close examination cleared that the MOF particles with an average size of about 50 nm are uniformly distributed in membrane matrix. The presence of MOF particles with definite channel size in membrane matrix can provide a new path and facile the passing of definite gases' and difficult the passing of others through the membrane. As a result, the membrane's selectivity and separation factors would be affected.

Gas permeation

During the addition of polymer to the solution, the critical concentration must be considered. For successful separation of gas, a thick selective layer in the membrane must be created by the incorpo-

Fig.7a, penetrant permeability in the PDMS membrane decreases in the following order: NO>O_2>N_2

Penetrant permeability is the product of diffusion coefficient and solubility. In weakly size sieving rubbery polymers such as PDMS, diffusion coefficients often change less than solubility coefficients among a group of penetrants so that more soluble penetrants are more permeable. Moreover, the critical temperature is frequently used as a scaling factor for penetrant condensability [24]. Generally, penetrants with higher critical temperatures are more soluble in polymers. According to Table 1, in this study, the expected correlation between the critical temperature of penetrant and its permeability is confirmed. Besides, there is a strong correlation between critical volume as a convenient average measurement of penetrant size and transport properties. As shown in Fig.7a, an increase in the critical volume of penetrants leads to a decrease in permeability which is consistent with previous research findings [25].

As shown in Fig.7a-h, the pressure of feed increases the permeability of penetrants. The pressure of feed can be affected the permeability by changing the three factors: penetrant diffusivity, free volume amount, and penetrant solubility. An increase

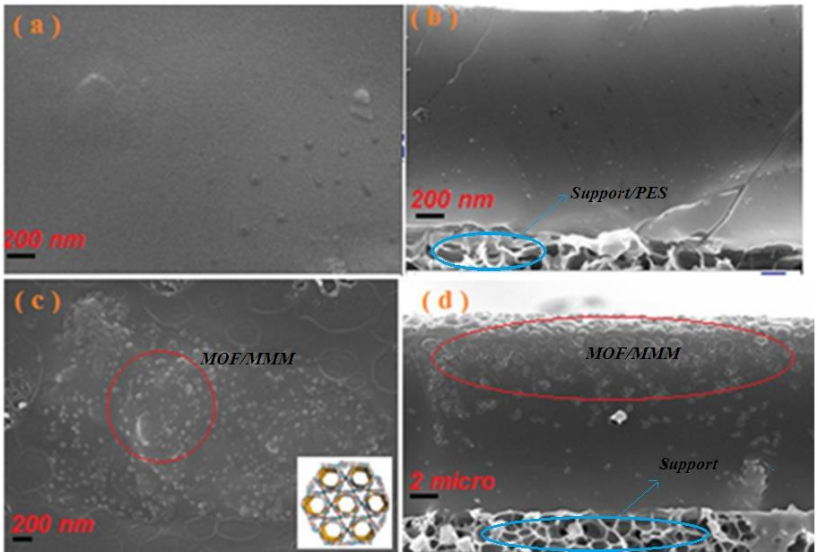

Fig. 6. SEM image of a) surface of PDMS/PES, b) cross section of PDMS/PES, c) surface MMM with 20wt% of nano Dy-BTC, d) Cross section of MMM with 20wt% of nano Dy-BTC.

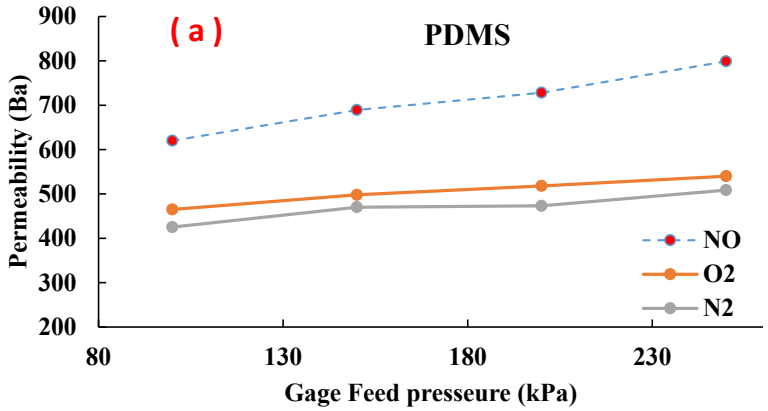

Fig.7 Effect of MOF loading in MMM on permeability (a,c,e and g) and selectivity (b, d, f and h) of NO, N_2 and O_2 at 100-250 kPa feed pressure.

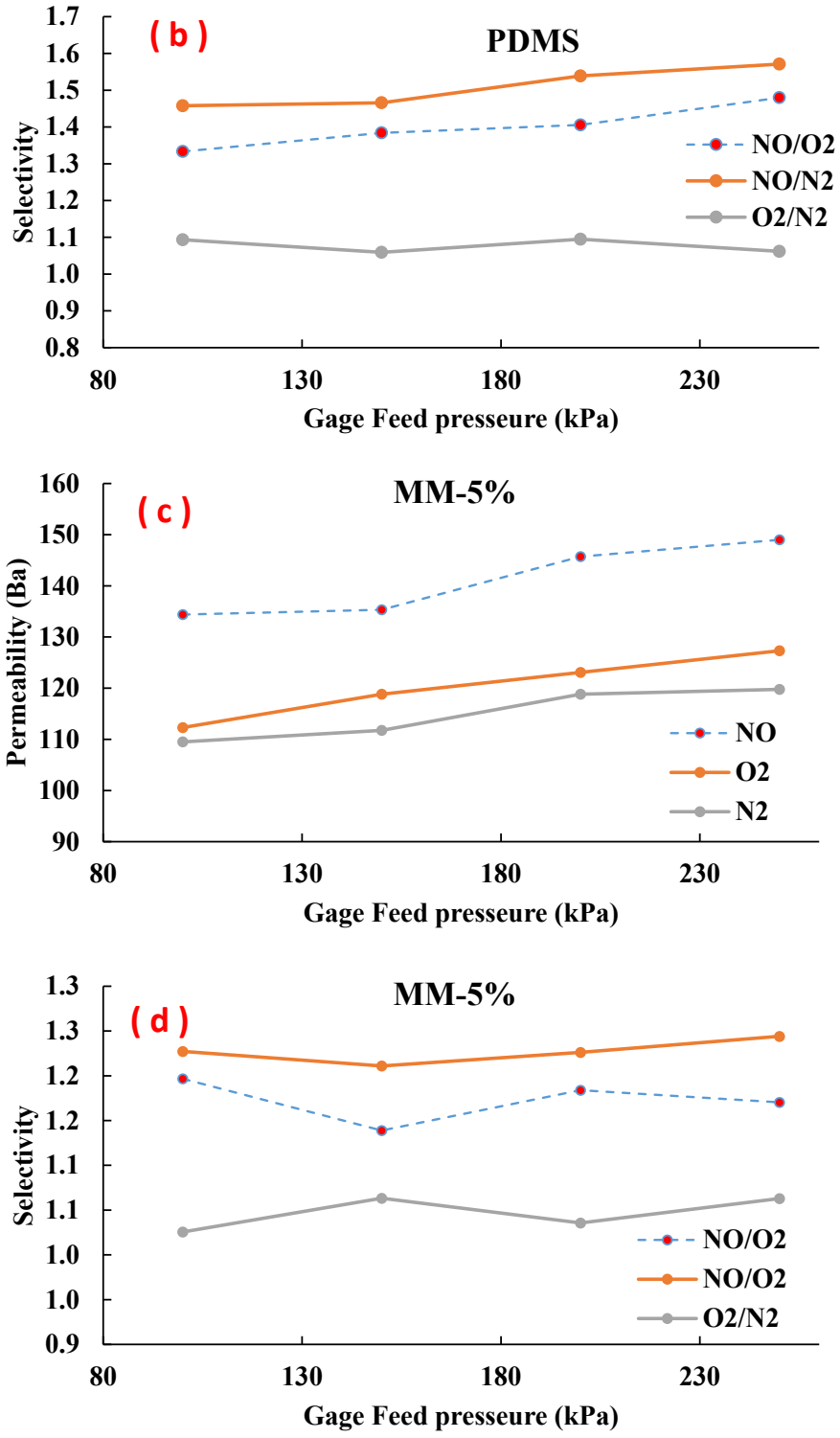

Continued Fig.7 Effect of MOF loading in MMM on permeability (a,c,e and g) and selectivity (b, d, f and h) of NO, N_2 and O_2 at 100-250 kPa feed pressure.

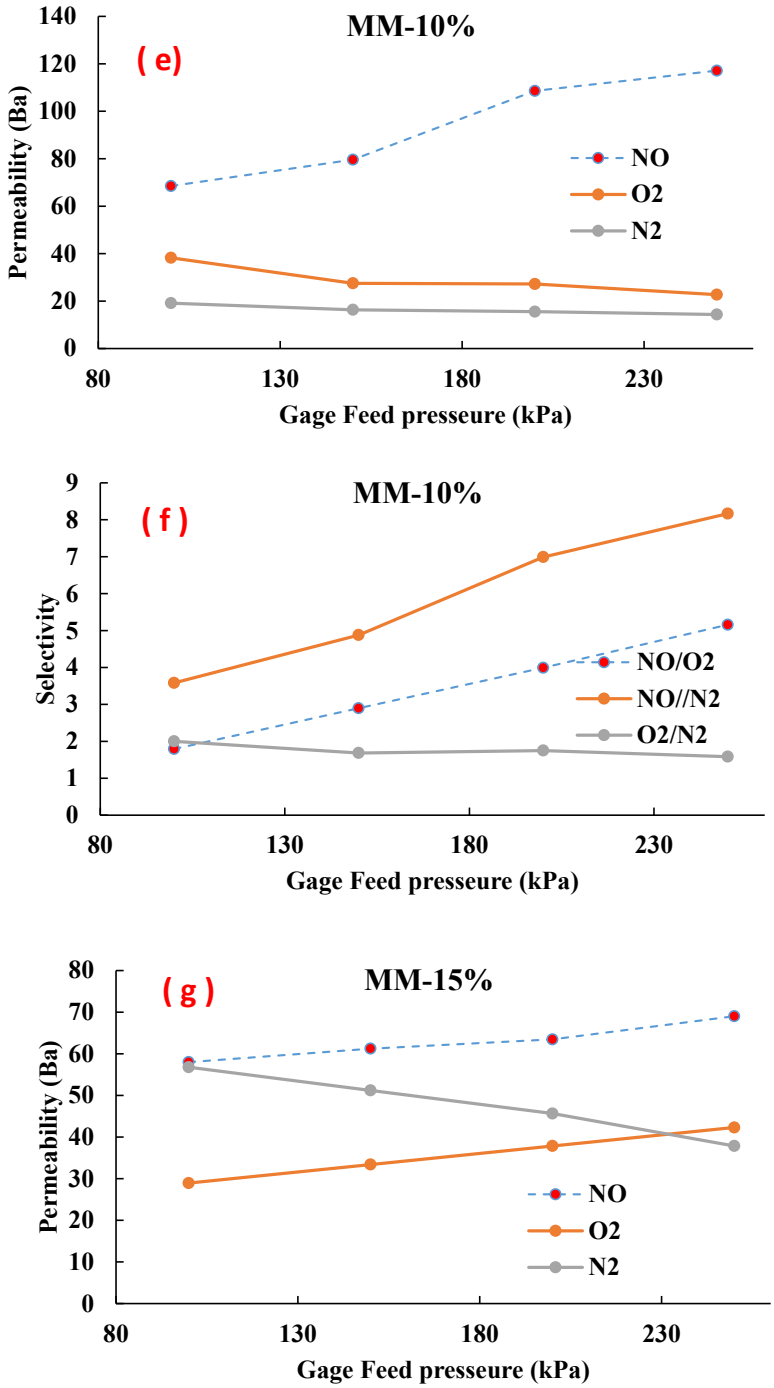

Continued Fig.7 Effect of MOF loading in MMM on permeability (a,c,e and g) and selectivity (b, d, f and h) of NO, N_2 and O_2 at 100-250 kPa feed pressure.

ration of chains. Based on researches the best concentrations of the polymer in the solvent are considered to be between 20 and 30 wt% [11, 22,23]. In the current work, the 30 wt% of the polymer in the solvent is chosen as the best composition for casting solution.

The effect of MOF loading on the membrane performance

Fig. 7(a-h), shows the permeability and selectivity of NO, N_2, O_2 gases as a function of loading Dy-BTC(0–15 wt%) in mixed matrix membrane at different feed pressure (100-250 kPa). As shown in

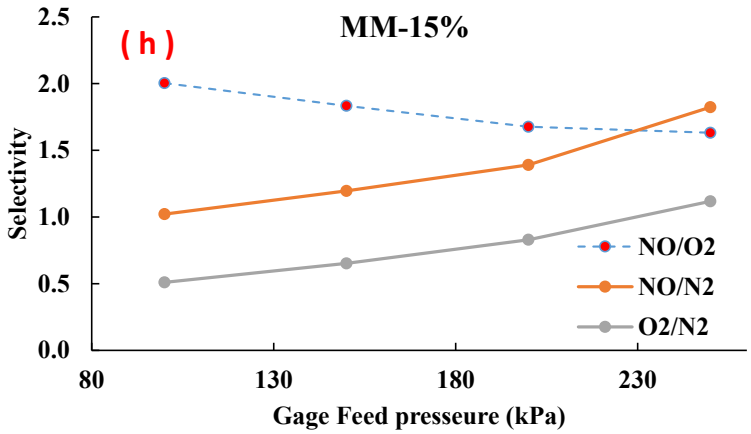

Continued Fig.7 Effect of MOF loading in MMM on permeability (a,c,e and g) and selectivity (b, d, f and h) of NO, N_2 and O_2 at 100-250 kPa feed pressure.

Table 1. Penetrant Critical Temperatures, Critical Volumes [26]

Gas	Tc (K)	Vc (cm^3/mole)
O_2	154.58	73.4
N_2	126.2	89.8
NO	180	58

in pressure leads to an increase in the solubility and diffusivity of penetrant molecules. As penetrant pressure and, therefore, penetrant concentration in the polymer increase, the tendency of the penetrant to diffuse inside the polymer matrix increases. On the other hand, high penetrant pressure can slightly compress the polymer matrix, thereby reducing the amount of free volume available for penetrant transport and reducing penetrant diffusion coefficients. Also, penetrant solubility in rubbery polymers frequently increases with pressure, leading to a corresponding increase in permeability. As a result of the interaction between these factors, the permeability coefficients of N_2, O_2, and NO penetrants, increase very slightly with increasing penetrant pressure.

The incorporation of MOF nanoparticles into the polymer structure leads to an improvement in selectivity at the expense of permeability due to a loss in free volume (Fig.7c-h). However, this effect is not significant for low MOF loading (5 %). The gas solubility in the membrane [22-30] and gas interaction with MOF are two important factors that affect on permeability and selectivity of MMM. Higher selectivities were found for NO compared to the N_2 and O_2. This could be attributed to the polar nature of NO. The strong interaction of NO gas with electrostatic fields of MOFs increased the solubility and diffusivity of NO in the membrane. The Van der Waals forces dominate the interaction between the nonpolar guest molecules and the building units of the MOFs, where chemical reaction involving electron transfer occurs upon adsorption of reactive species such as polar molecules. NO adsorption has been studied before [27], showing that NO interacts strongly with metal centers. The optimum loading amount of MOF to achieving high selectivity at 250 kPa feed pressure was 10 % MOF (Fig.7f).

CONCLUSION

The new metal-organic framework was synthesized in this research. The product was characterized by XRD, TG, BET, and SEM techniques. The XRD pattern confirms the successful synthesis of Dy-BTC MOF. The surface area was 801.033 m^2/g with a total pore volume of 1300 cc $g^{-1}(p/p^\circ = 0.98$. Mixed-matrix membranes (MMMs) comprised of polydimethylsiloxane (PDMS) as continuous,

MOF as the dispersed phase, and polyethersulphone (PES) as support have been prepared to investigate NO, N_2, and O_2 separation. The effect of MOF nanoparticles and feed pressure on permeability and selectivity were studied. The NO/N_2 and NO/O_2 selectivities increased with MOF particles increasing in the polymer matrices. The feed pressure has no important effect on separation factors. The results indicated that the addition of MOF nanoparticles to the membrane aiming the NO gas separation.

CONFLICTS OF INTEREST

The authors declare that there are no conflicts of interest.

REFERENCES

1. Barea E, Montoro C, Navarro JAR. Toxic gas removal – metal–organic frameworks for the capture and degradation of toxic gases and vapours. Chem Soc Rev. 2014;43(16):5419-30.
2. Bowman CT. Kinetics of pollutant formation and destruction in combustion. Prog Energy Combust Sci. 1975;1(1):33-45.
3. Baukal C. Everything you need to know about NOx: Controlling and minimizing pollutant emissions is critical for meeting air quality regulations. Met Finish. 2005;103(11):18-24.
4. Hussain M, König A. Mixed-Matrix Membrane for Gas Separation: Polydimethylsiloxane Filled with Zeolite. CHEM ENG TECHNOL. 2012;35(3):561-9.
5. Nunes SP, Peinemann K-V. Membrane technology: Wiley Online Library; 2001.
6. Chung T-S, Jiang LY, Li Y, Kulprathipanja S. Mixed matrix membranes (MMMs) comprising organic polymers with dispersed inorganic fillers for gas separation. Prog Polym Sci. 2007;32(4):483-507.
7. Chuah CY, Bae T-H. Incorporation of Cu3BTC2 nanocrystals to increase the permeability of polymeric membranes in O2/N2 separation. BMC Chemical Engineering. 2019;1(1):2.
8. Salleh WNW, Ismail AF. Carbon membranes for gas separation processes: Recent progress and future perspective. Journal of Membrane Science and Research. 2015;1(Issue 1):2-15.
9. Aykac Ozen H, Ozturk B. Gas separation characteristic of mixed matrix membrane prepared by MOF-5 including different metals. Sep Purif Technol. 2019;211:514-21.
10. Lin R, Villacorta Hernandez B, Ge L, Zhu Z. Metal organic framework based mixed matrix membranes: an overview on filler/polymer interfaces. J Mater Chem A. 2018;6(2):293-312.
11. Chevinly AS, Mobtaker HG, Yousefi T, Shirani AS, Aghayan H. {[Ce(BTC)(H2O)]·DMF}n metal organic framework as a new adsorbent for removal of neodymium ions. Inorg Chim Acta. 2017;455:34-40.
12. Leonard R. MacGillivray (Editor) CMLE. Metal-organic framework materials: John Wiley & Sons; 2014. 592 p.
13. Tanh Jeazet HB, Staudt C, Janiak C. Metal–organic frameworks in mixed-matrix membranes for gas separation. Dalton Trans. 2012;41(46):14003-27.
14. Amiri H, Charkhi A, Moosavian MA, Ahmadi SJ, Nourian H. Performance improvement of PDMS/PES membrane by adding silicalite-1 nanoparticles: separation of xenon and krypton. Chemical Papers. 2017;71(9):1587-96.
15. Abbasi A, Moradpour T, Van Hecke K. A new 3D cobalt (II) metal–organic framework nanostructure for heavy metal adsorption. Inorg Chim Acta. 2015;430:261-7.
16. Yousefi T, Mostaedi MT, Ghasemi M, Ghadirifar A. A Simple Way to Synthesize of Samarium Oxide Nanoparticles: Characterization and Effect of pH on Morphology. Synthesis and Reactivity in Inorganic, Metal-Organic, and Nano-Metal Chemistry. 2016;46(1):137-42.
17. Wang H-L, Yeh H, Chen Y-C, Lai Y-C, Lin C-Y, Lu K-Y, et al. Thermal Stability of Metal–Organic Frameworks and Encapsulation of CuO Nanocrystals for Highly Active Catalysis. ACS Appl Mater Interfaces. 2018;10(11):9332-41.
18. Yousefi T, Torab-Mostaedi M, Moosavian MA, Mobtaker HG. Potential application of a nanocomposite:HCNFe@ polymer for effective removal of Cs (I) from nuclear waste. Prog Nucl Energy. 2015;85:631-9.
19. Israr F, Chun D, Kim Y, Kim DK. High yield synthesis of Ni-BTC metal–organic framework with ultrasonic irradiation: Role of polar aprotic DMF solvent. Ultrason Sonochem. 2016;31:93-101.
20. Nie P, Shen L, Luo H, Li H, Xu G, Zhang X. Synthesis of nanostructured materials by using metal-cyanide coordination polymers and their lithium storage properties. Nanoscale. 2013;5(22):11087-93.
21. Peng MM, Ganesh M, Vinodh R, Palanichamy M, Jang HT. Solvent free oxidation of ethylbenzene over Ce-BTC MOF. Arabian J Chem. 2019;12(7):1358-64.
22. Moermans B, Beuckelaer WD, Vankelecom IFJ, Ravishankar R, Martens JA, Jacobs PA. Incorporation of nano-sized zeolites in membranes. Chem Commun. 2000(24):2467-8.
23. Wallace DW, Staudt-Bickel C, Koros WJ. Efficient development of effective hollow fiber membranes for gas separations from novel polymers. J Membr Sci. 2006;278(1):92-104.
24. missing.
25. Merkel TC, Bondar VI, Nagai K, Freeman BD, Pinnau I. Gas sorption, diffusion, and permeation in poly(dimethylsiloxane). J Polym Sci, Part B: Polym Phys. 2000;38(3):415-34.
26. Reid RC, Prausnitz JM, Poling BE. The properties of gases and liquids. 1987.
27. Tan K, Chabal YJ. Interaction of Small Molecules within Metal Organic Frameworks Studied by In Situ Vibrational Spectroscopy: InTechOpen; 2016.
28. Nour M, Berean K, Griffin MJ, Matthews GI, Bhaskaran M, Sriram S, et al. Nanocomposite carbon-PDMS membranes for gas separation. Sens Actuators, B. 2012;161(1):982-8.
29. Porter MC. Handbook of industrial membrane technology. 1989.
30. Wu F, Li L, Xu Z, Tan S, Zhang Z. Transport study of pure and mixed gases through PDMS membrane. CHEM ENG J. 2006;117(1):51-9.